Geomechanical and Petrophysical interpretation in Shale formations: A case study in Pimienta, México.

Jesús P. Salazar*[1], Douglas J. Betancourt[3], Claudio Rabe[1], Omer Lqbal[2], and Eugenia Sardelli[4]. [1]Baker Hughes, [2]Petronas University, [3]Central University of Venezuela (UCV), [4]University of Oriente (UDO).

Abstract

Currently, shallow and light-oil reservoirs can be difficult to find out in Mexico. For this reason, oil and gas operators are exploring and developing complex, risky and therefore costly reservoirs such as unconventional plays of oil and gas shale. This is the case of the Pimienta Formation, located in the southern portion of the Burgos basin in Mexico, which has been identified as a good potential source rock to become a shale oil producer. This study presents a petro-technical assessment and evaluation in the Pimienta formation, integrating petrophysical and rock physics models by using a dataset from one well characterized with complete logs. The petrophysical model include rock properties such as porosity, permeability and pore throat radius and the geomechanical model is based on brittleness, which is estimated from a combination between Young's modulus and Poisson's ratio. All these properties are evaluated together to determine the best intervals for hydraulic stimulation.

Introduction

The integration of petrophysical and geochemical models has been proved being very important to define a successful strategy to determine the sweet spot interval for production optimization in unconventional reservoirs. This integration is also important for defining completion fluid, required surface pressure to stimulate and the optimum production well length (Paris et. al).

In this study, optimum stimulation design analysis began by collecting available information in Well-A from early Jurassic Formation in Burgos basin (Figure 1). Conventional and NMR well logs were used to model 1-D profiles of mineralogy, porosity, permeability, TOC and elastic parameters, which were calibrated and validated with core analysis performed in the laboratory. These models are then used to understand the pore throat radius distribution, lithology, TOC quantification and rock brittleness to identify the best zones for hydraulic fracturing stimulation.

Figure 1. Study area location.

Pore throat radius calculation is based on the mathematical models developed by Pittman (1992) which offer a valid approach to estimate this property from porosity and permeability. This approach can be used to determine a petrophysical classification based on the quality of the pore system and in the flow through the pore space. The best Pittman's model to calculated pore throat radius is defined from mercury injection analyses performed in core samples.

Total organic content (TOC) calculation is based on the Passey equation, which considers a combination between resistivity and compressional velocity with the integration of rock maturity data (Passey et al., 1990).

Brittleness calculation is based on the Rickman et. al (2008) methodology, which they suggest that the brittleness concept should combine Poisson's ratio and Young's modulus derived from acoustic log data. Their model assumes that rocks with high brittleness show high Young's modulus and low Poisson's ratio. Consequently, rocks with low brittleness show low Young's modulus and high Poisson's ratio.

This study considers a combined analysis between pore throat radius, TOC and rock brittleness to determine the best interval to execute hydraulic fracturing operations. This results of the fracturing operation are shown to confer the quality of the selected interval.

Method

The available well log information for the Well-A in the Pimienta formation includes gamma ray, resistivity, neutron porosity, bulk density, acoustic velocity and nuclear magnetic resonance (NMR) logs. Porosity and

permeability are calibrated with core samples analysis performed in the laboratory as displayed in Figure 2.

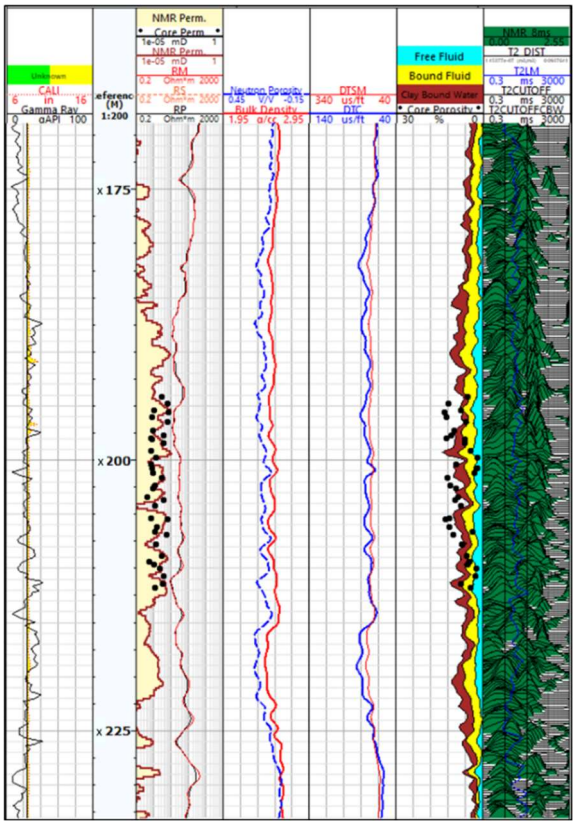

Figure 2. Available well log information for Well-A.

The comparison between NMR permeability with core sample permeability is displayed in the third track of Figure 2. It can be noticed a good correlation between laboratory measurements and the estimated profile. Similarly, the comparison between NMR porosity with porosity obtained from core samples in the sixth track of Figure 2 is also showing a good correlation between them.

In terms of geomechanical properties, brittleness describe the ability of a rock to respond to the initiation and propagation of a fracture and is one of the keys for identifying ideal perforating intervals.

Rickman et al. (2008) suggest that brittleness concept should combine the Young's modulus and Poisson's ratio because brittle rocks have higher Young's modulus and lower Poisson's ratio. So, a brittleness index (BI) can be generated considering these geomechanical charactetistics of a brittle rock. They proposed the following equation:

$$BI = 0.5\left[\frac{E_v - E_{min}}{E_{max} - E_{min}} + \frac{\nu_v - \nu_{max}}{\nu_{min} - \nu_{max}}\right] \qquad (1)$$

where E_v is the average Young's modulus, E_{min} and E_{max} are minimum and maximum Young's modulus respectively, $\boldsymbol{\nu}_v$ is the average Poisson's ratio and $\boldsymbol{\nu}_{min}$ and $\boldsymbol{\nu}_{max}$ are the minimum and maximum Poisson's ratio respectively.

Young's modulus is obtained from acoustic log data, specifically from formation compressional velocity as described in the next equation:

$$Ym = \rho V_s^2 \frac{3V_p^2 - 4V_s^2}{V_p^2 - V_s^2} \qquad (2)$$

where ρ is the bulk density, V_p is the compressional velocity and V_s is the shear velocity.

Poisson's ratio is also obtained from acoustic log data as described in the next equation:

$$Pr = \frac{V_p^2 - 2V_s^2}{2(V_p^2 - V_s^2)} \qquad (3)$$

In terms of petrophysical evaluation, the total organic content (TOC) is calculated using the Passey equation, which considers a combination between resistivity and compressional velocity with the integration of rock maturity data and the proper definition of baseline and can be expressed as (Passey et al., 1990).

$$\Delta\, logR_t = log_{10}\left(\frac{R}{R_{baseline}}\right) + 0.02 * (\Delta t - \Delta t_{baseline}) \qquad (4)$$

Where $\Delta\, logR_t$ is the curve separation measured in logarithmic resistivity cycles, R is the measured resistivity, Δt is the P wave transit time , $R_{baseline}$ is the resistivity corresponding to $\Delta t_{baseline}$ value when the logs are taken in non-source, clay-rich rocks. The empirical Passey equation for calculating TOC in clay-rich rock from ΔlogRt is (Passey et al, 1990):

$$TOC = \Delta logR_t * 10^{(2.297 - 0.1688 * LOM)} \qquad (5)$$

where TOC is the total organic content and LOM is the maturity.

In another hand, pore throat size is the circle drawn perpendicular to the flow direction in the narrowest point in the connection between two nearest pores (Salazar, 2007). The pore size is the radius of the biggest sphere that can be placed inside the pore. Windland (1975) developed a correlation to calculate pore throat radius from porosity and permeability. This correlation is described as:

$$logr_{35} = 0.732 + 0.588\log(k_{air}) - 0.864\log(\phi) \qquad (6)$$

where r_{35} is the pore throat radius at 35 % of mercury saturation, k_{air} is the rock permeability and ϕ is the rock porosity.

Later, Pittman (1992) developed a group of empirical equations to calculate pore throat radius from 10 % to 75 % of mercury saturation. These equations are described as:

$$logr_{10} = 0.459 + 0.500\log(k_{air}) - 0.385\log(\phi)$$
$$logr_{15} = 0.330 + 0.509\log(k_{air}) - 0.344\log(\phi)$$
$$logr_{20} = 0.218 + 0.519\log(k_{air}) - 0.303\log(\phi)$$
$$logr_{25} = 0.204 + 0.531\log(k_{air}) - 0.350\log(\phi)$$
$$logr_{30} = 0.215 + 0.547\log(k_{air}) - 0.420\log(\phi)$$
$$logr_{35} = 0.255 + 0.565\log(k_{air}) - 0.523\log(\phi)$$
$$logr_{40} = 0.360 + 0.528\log(k_{air}) - 0.680\log(\phi)$$
$$logr_{45} = 0.609 + 0.608\log(k_{air}) - 0.974\log(\phi)$$
$$logr_{50} = 0.778 + 0.626\log(k_{air}) - 1.205\log(\phi)$$

$$logr_{55} = 0.948 + 0.632\log(k_{air}) - 1.426\log(\phi)$$
$$logr_{60} = 1.096 + 0.648\log(k_{air}) - 1.666\log(\phi)$$
$$logr_{65} = 1.372 + 0.643\log(k_{air}) - 1.979\log(\phi)$$
$$logr_{70} = 1.664 + 0.627\log(k_{air}) - 2.314\log(\phi)$$
$$logr_{75} = 1.880 + 0.609\log(k_{air}) - 2.626\log(\phi)$$

The optimal Pittman equation for the formation is selected using the apex plot method, which is obtained from the results of mercury injection in the laboratory that consists in injecting mercury into the samples to different pressures. A crossplot between mercury saturation divided by injection pressure vs mercury saturation is presented. The maximum of each curve corresponds to the dominant pore throat radius that is related to certain mercury saturation as shown in Figure 3.

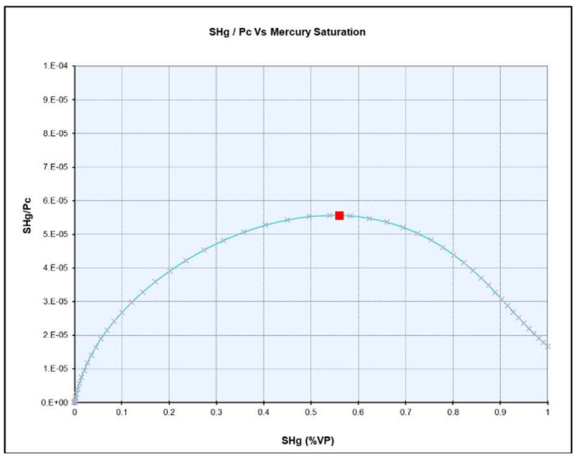

Figure 3. Apex plot for a simple core sample.

This curve is done for the whole sample set and a global maximum is determined. Based on this global maximum, the dominant mercury saturation is selected and so the best Pittman equation for the formation. Once the equation is selected, the pore throat size calculation is performed and the best zones, in terms of fluid flow, are determined.

Once brittleness and pore throat radius are estimated, a geomechanical and petrophysical classification is performed.

The geomechanical classification is based on brittleness, which describes the ability of the rock to respond to hydraulic fracturing and propagation. This property support the identification of the ideal fracturing intervals. Additionally, the petrophysical classification is based on the quality of the rock in terms of fluid flow through the pore space. Rocks with the higher pore throat size are supposed to be better for the fluid flow. Both properties are analyzed together in order to improve the selection of the best intervals for hydraulic stimulation.

Results

As mentioned before, the information available includes petrophysical well logs and core samples analysis performed in the laboratory. The laboratory analysis includes porosity and permeability estimation as well as capillary pressure by mercury injection.

For geomechanical interpretation, Brittleness index (BI) was estimated as indicator of the best zones for hydraulic fracturing. This property was estimated using the Eq. 1, which related BI with Young's modulus and Poisson's ratio that were calculated from Eq. 2 and 3 respectively. The minimum and maximum value of Young's modulus and Poisson's ratio were obtained from histogram for both properties. Figure 4 shows the histogram for Young's modulus and Figure 5 for Poisson's ratio.

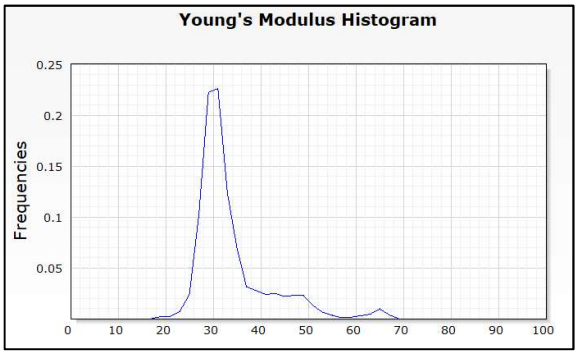

Figure 4. Young's modulus histogram for Pimienta formation.

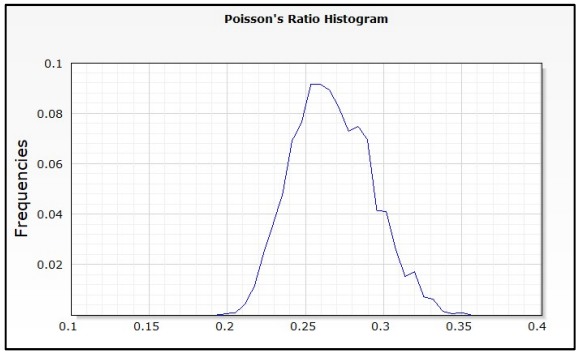

Figure 5. Poisson's ratio histogram for Pimienta formation.

Based in these histograms, the minimum and maximum value for Young's modulus were determined in 15 and 75 GPa respectively. Additionally, the minimum and maximum value of Poisson's ratio were determined in 0.2 and 0.35 respectively. All these values were used to determine brittleness index from Eq. 1. The result of this combination is displayed in the crossplot between Young's modulus and Poisson's ratio of Figure 6. The crossplot is colored by the estimated brittleness index.

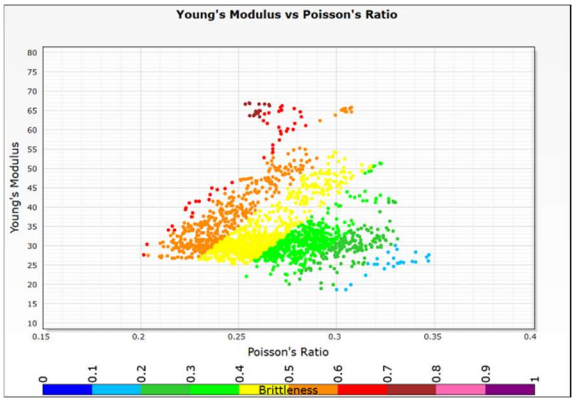

Figure 6. Young's Modulus vs Poisson's Ratio Crossplot for Pimienta formation.

Based on the concept of brittleness that defines that the most brittle material shows high Young's modulus and low Poisson's ratio, the most brittle material is located in the northwest quadrant in the crossplot of Figure 6 as indicated by the color bar. A continued brittleness curve, estimated from Young's modulus and Poisson's ratio is shown in the seventh track of the Figure 7. It is also included Young's modulus and Poisson's ratio in fifth and sixth track respectively.

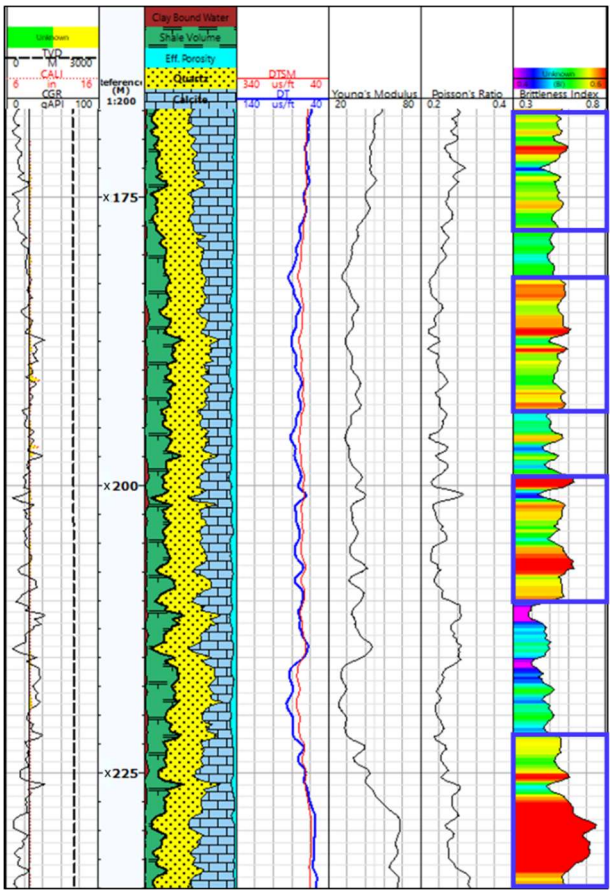

Figure 7. Geomechanical Interpretation for Well-A, including Young's Modulus, Poisson's Ratio and Brittleness.

Based on the geomechanical interpretation shown in Figure 7, the best relative interval, in terms of brittleness is between x222 and x235 meters, indicating the best rock for fracturing. Other intervals that could be also considered for fracturing, based on brittleness, are between x167 and x178, between x182 and x193, x199 and x210 (blue boxes).

Beside to brittleness, an important petrophysical parameter to be evaluated for the selection of the optimal intervals for hydraulic fracturing is the total organic carbon (TOC), which was calculated using Passey's methodology. The TOC is an indicator of the presence of hydrocarbon in the shale formation. High TOC indicates a higher content of hydrocarbon and vice versa.

It is important, to include the TOC in the crossplot between Young's modulus and Poisson's ratio. Figure 8 shows a crossplot between Young's Modulus and Poisson's ratio colored by TOC. The lines in the crossplot represent the limits for Brittleness from 0.1 to 0.9.

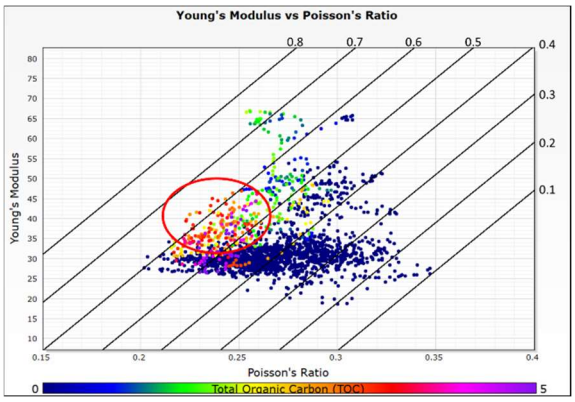

Figure 8. Young's Modulus vs Poisson's Ratio Crossplot colored by TOC for Pimienta formation.

To select the best intervals for hydraulic fracturing, brittleness needs to be combined with TOC. Therefore, intervals with the highest brittleness and high TOC are the best candidates to be fractured. These intervals corresponds to the points circled in red in the Figure 8, which have high brittleness but also high TOC.

For another hand, the data from mercury injection analysis was used to determine the best Pittman equation for Pimienta formation using the apex method that consists in plotting a crossplot between the injected mercury saturation divided by the capillary pressure and the injected mercury saturation itself for some of the available core samples. The results are shown in Figure 9.

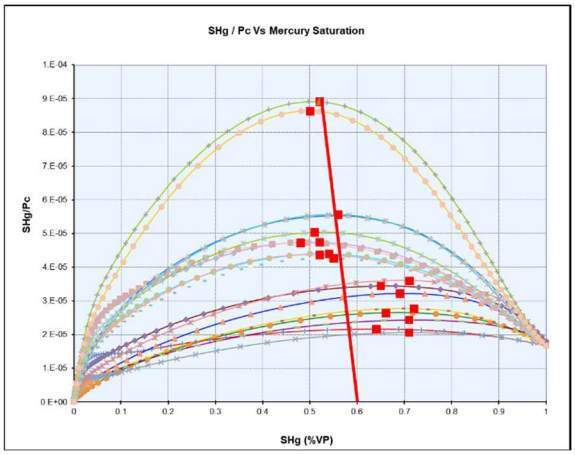

Figure 9. Apex plot for all available core samples.

It can inferred that the pore throat radius that dominates de fluid flow for this group of samples corresponds to 60 % of mercury saturation. So, the equation used to estimated pore throat radius is:

$$logr_{60} = 1.096 + 0.648\log(k_{air}) - 1.666\log(\phi) \qquad (5)$$

Using the available NMR log data, which includes porosity and permeability that were calibrated with laboratory analysis performed in core samples, and using Eq. 5, a continuous curve of pore throat radius can be performed. The results are displayed in Figure 9.

A continued curve of brittleness, TOC and and pore throat radius is displayed in the Figure 10. It is also included the total porosity curves calibrated with core samples porosities as well as Young's modulus and Poisson's ratio. The calculated TOC is compared with the TOC measured in core samples using pyrolysis in the eighth track, showing a good correlation between them.

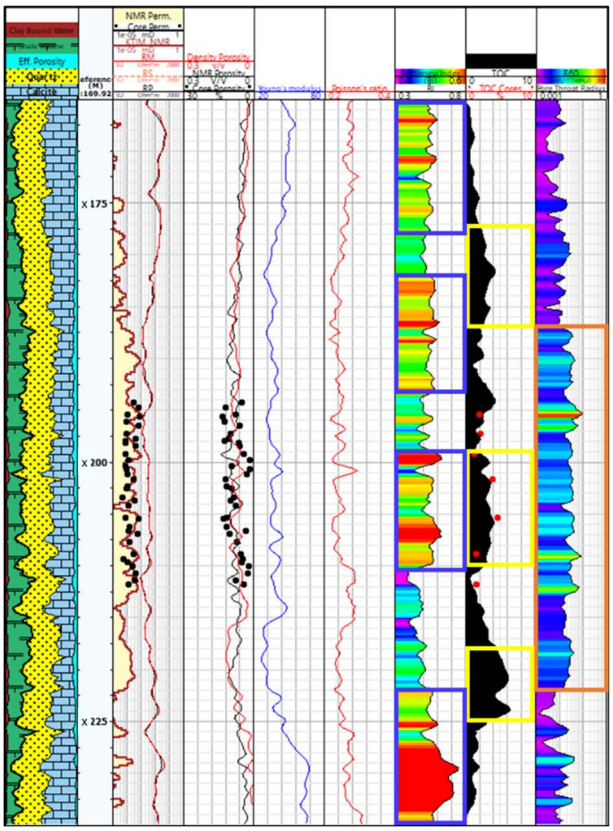

Figure 10. Geomechanical and petrophysical Interpretation for Well-A, including Young's Modulus, Poisson's Ratio, Brittleness, TOC and pore throat radius.

Based on the petrophysical interpretation shown in Figure 10, it can be noticed that the best relative intervals, in terms of TOC, would be between x177 and x187 meters, between x199 and x210 meters and between x218 and x225 meters (yellow boxes in Figure 10). These intervals show a relative higher TOC, which is favorable for hydrocarbon production. In terms of pore throat radius, the best interval is between x187 and x222 meters (orange box in Figure 10), indicating a better rock quality to allow the fluid flow.

Selecting the best intervals for hydraulic stimulation should consider an integration between brittleness, TOC and pore throat radius. In terms of brittleness and TOC, the best intervals are those with high brittleness and high TOC to guarantee fracture propagation and hydrocarbon production. Now, in terms of pore throat radius, the intervals to be considered for fracturing should be those with high total porosity, which guarantee the presence of hydrocarbon, and high pore throat radius. Based on it, the best interval should be between x199 and x210 as shown in Figure 11 (Red box).

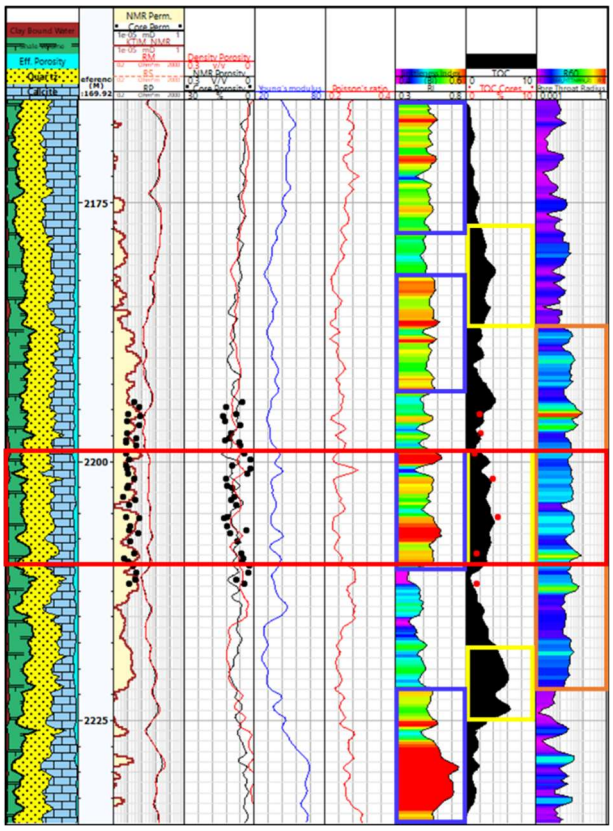

Figure 11. Best intervals for hydraulic fracturing for Well-A indicated by red boxes.

These optimum interval for stimulation was able to successful induce fractures with larger fracture length, length to height 1/0.40. The average fracture conductivity indicates 166 mD-ft, a fracture width of 0.12 inches and a fracture length of 187 meters. These results show an improvement when compare with the results from hydraulic fracturing performed in the upper interval in correlate wells, which show an average fracture conductivity of 67 mD-ft, a fracture width of 0.07 inches and a fracture length of 180 meters. It also an improvement when compared with the results from the lower interval, which show an average fracture conductivity of 83 mD-ft, a fracture width of 0.08 and a fracture length of 182 meters. The results are summarized in Table 1.

Table 1. Post-Fracturing results in different intervals

Interval	Fracture Conductivity	Fracture width (in)	Fracture length (m)
Optimum	166	0.12	187
Upper	67	0.07	180
Lower	83	0.08	182

Conclusions

The results indicate that the best intervals for reservoir stimulation in the Pimienta formation is in the middle of the study formation, where the high amount of TOC, high pore pressure, median Young's modulus, low Poisson's ratio and High porosity, indicate good reservoir quality and an

excellent interval for reservoir stimulation in order to improve the connectivity between the pores allowing the hydrocarbon production. This is confirmed when the results of the hydraulic fracturing are analyzed and compared with the results of hydraulic fracturing in the other intervals performed in correlate wells.

Acknowledgments

The authors wish to thank and acknowledge PEMEX for granting access to use their data, CNH for permission to publish the results from the study and Baker Hughes for providing the software license to execute the analysis.

References

FATAH, T. Y. A., RABE, C., SALAZAR, J. P.; RECHDEN FILHO, R. C., (2016), "Estimating Brittleness Index Using Mineralogy and TOC in the Whangai Formation, New Zealand", Paper IBP1956_16, Rio Oil & Gas Expo and Conference, 24-27 October.

HUCKA, V., DAS, B., Brittleness determination of rocks by different methods. Int. J. Rock Mech. Min. Sci. & Geomech. Abstr. 11: 389-92, 1974.

JARVIE, D. M., R. J., HILL, T. E., RUBLE, AND POLLASTRO, R. M., Unconventional shale -gas systems: The Mississippian Barnett Shale of north-central Texas as one model for thermogenic shale –gas assessment: AAPG Bulletin, 91, no. 4, 475–499, 2007.

PARIS, M., RABE, C., FILHO R.R., SALAZAR, J.P. (2016). Application of geomechanical concepts in oriented perforating design in Whangai Formation, East Coast of New Zealand. Latin American Perforating Symposium. Buenos Aires, Argentina.

PASSEY, Q. R., CREANEY, S., KULLA, J.B., MORETTI, F.J. and STROUD, J.D. (1992). A practical model for organic richness from porosity and resistivity logs. The American Association of Petroleum Geologists Bulletin. December 1990.

PITTMAN E. (1992). Relationship of porosity and permeability to various parameters derived from mercury injection capilary pressure curves for sandstone. AAPG bulletin, V76, Nº 2. Tulsa. USA.

PORRAS J. C. (1998). Determination fo rock types from Pore throat radius and bulk volume water and their Relation to lithofacies, carito north field, Venezuela BASIN. SPWLA 39th Annual logging symposium.

PORRAS J. C and CAMPOS, O. (2001). Rock typing: a key for petrophysical characterization and definition of flow units, santa bárbara field, eastern venezuela basin. SPE 69458. Buenos Aires. Argentina.

RABE, C., SALAZAR, J.P., RECHDEN FILHO, R. C., PASQUA, F. (2021). Brittleness modeling selects optimum stimulation zone in shale source rocks in the Whangai Formation, New Zealand. AAPG Bulletin, V105.

RICKMAN, R., MULLEN, M., PETRE, E., GRIESER, B. and KUNDERT, D., (2008). A practical use of shale petrophysics for stimulation design optimization: All shale plays are nor clones of the Barnett Shale. SPE 115258, Proc. Ann. Tech. Conf., Denver, Co.

ROMERO, P. A., BRUZUAL, G and SUÁREZ, O. (2002). Determination of rock quality in sandstone core plug samples usin NMR. SCA 2002-51. Monterrey, USA.

SALAZAR, J.P., MORILLO, B., (2007). Pore throat size classification from Nuclear Magnetic Resonance measurements in rocks. 10th International Congress of the Brazilian Geophysical Society. Rio de Janeiro, Brazil.

SALAZAR., J. P.; RABE, C. and RECHDEN FILHO, R. C. (2017). "Some Effects of Petrophysics and Geomechanics in Unconventional Reservoir Stimulation, New Zealand". Paper UR38 First EAGE/AMGP/AMGE Latin-American Seminar in Unconventional Resources, 23-24 November, Mexico City, Mexico, 2017.

ZOBACK, M.,D., (2010)Reservoir Geomechanics, Cambridge University Press, 1st Edition, 2010.